

Supplementary data

PEG hydration and conformation in solution: hints to macromolecular crowding

S. Di Fonzo^a, B. Bellich^b, A. Gamini^c, N. Quadri^c, A. Cesàro^{a,c}

^a Elettra Sincrotrone Trieste, Area Science Park, I-34149 Trieste, Italy

^b Department of Life Sciences, University of Trieste, Via Giorgieri 1, 34127 Trieste, Italy

^c Department of Chemical and Pharmaceutical Sciences, University of Trieste, Via Giorgieri 1, 34127 Trieste, Italy

Figure S1. Melting temperature of PEG samples were $T_m = 21, 42$ and 63 °C (peak temperatures) for PEG 600, PEG 1000 and PEG 6000, respectively, and were determined by DSC measurement at 20 °C/min scanning rate. Crystallization peaks were displaced to low temperature and showed multiple peaks. The melting temperatures define the limits for using pure liquid PEG in spectroscopic measurements.

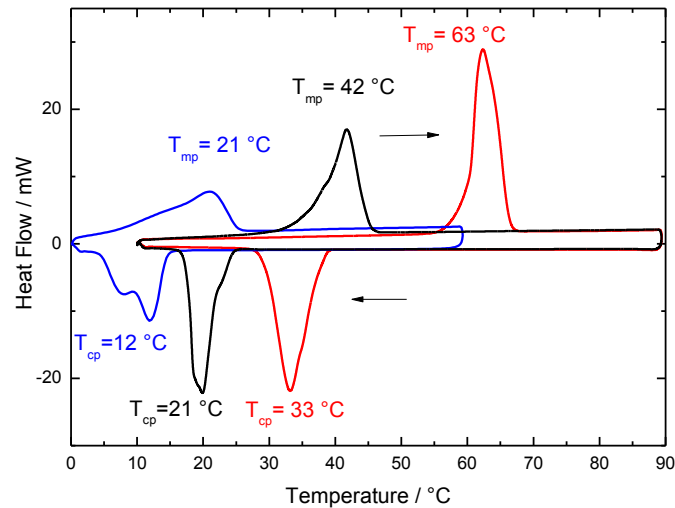
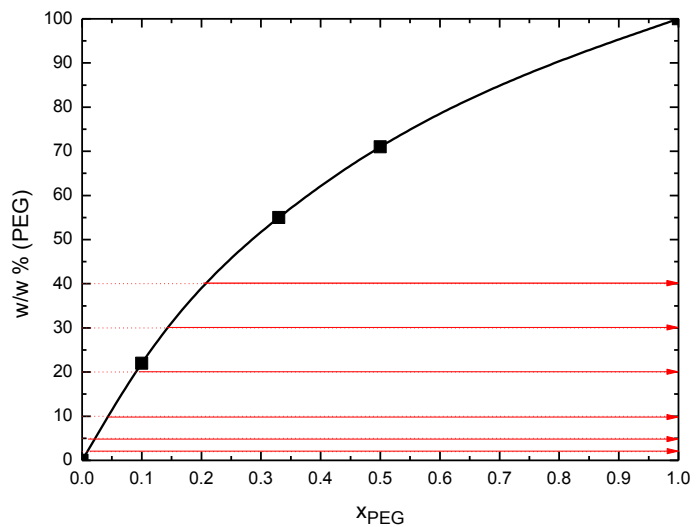


Table S1 and Figure S2. Synopsis of the PEG concentration used in the spectroscopic experiments expressed as monomer molar fraction (x) and weight % (w/w %). The Figure S2 shows the relation between the two concentration scales. The red horizontal arrows represent the range of concentration spanned in each calorimetric dehydration experiment from initial PEG concentration to fully dehydrated sample.

x (PEG)	w/w % (PEG)	x (H ₂ O)
0	0	1
0.10	21.36	0.90
0.33	55	0.667
0.50	70.97	0.50
1	100	0



Isothermal evaporation model and general shape of dehydration curves by calorimetry.

The experimental dehydration curves of aqueous solutions from thin films measured by a novel isothermal calorimetric method (Figure S3) follow a general trend such as the one reported in Figure S4. The phenomenological aspect of these typical curves is briefly described here, with the aim of identifying the three characteristic regions shown in the experimental isothermal dehydration curve in Figure S4. The region (A), called quasi-constant rate (qcr) region, is the true measure of the evaporative rate of a solution undergoing a continuous slow increase in solute concentration within the control of constant operative parameters discussed below. The region (B) shows a characteristic sigmoidal shape which corresponds to the decrease of water content to zero, with the concomitant final hardening of the residual anhydrous matrix. The peak in the region (C) describes the initial thermal perturbation of the calorimeter due to the insertion of the sample. This region is characterized by an exponential decay and overlaps the thermal evaporation signal in the very beginning of the calorimetric curve. The linear calorimetric signal underlying the region (C) can be easily reconstructed as shown in Figure S4 by extrapolating the value of the heat flow at $t = 0$ (HF_0).

Thus, once the value of $HF(t=0)$ has been correctly assigned to the value of a_w for the concentration at $t=0$, the actual evaporation process $HF(t)$ shown by the red full line in Figure S4 represents the true measure of the water activity (a_w) as a function of concentration.

It is worth resuming that the critical issue in the proposed evaporative model is to maintain constant the planar surface during the whole process of evaporation. Under these circumstances, the theory predicts a direct relation between the rate of water evaporation (measured by HF) and the water activity at the liquid surface, under constancy of the external parameters, temperature, pressure and relative humidity. The correlation is guaranteed by the mesoporous morphology of the thin paper filter, its capability of being largely imbibed and its insoluble nature. Furthermore, as long as the water diffusion within the system is larger than (or equal to) the evaporation rate, the system is under quasi-equilibrium conditions, providing the proportionality between water activity and HF. Under these conditions, the measurement of water activity as a function of water content of the system is continuously provided by the experimental heat flow curve.

Figure S3 shows the model (left), the set-up (center) and the «electro-thermal analogy» (right).

The simple hybrid diagram (right) describes the heat and water mass transfers in the calorimeter chamber. The suffixes of temperature T , of resistance R , mass m , and heat power Q , refer to the furnace F , sample s , reference r , and atmosphere a . In the inset, the scheme of water evaporation from a thin aqueous film of diameter d and thickness $L(t) \ll d$, deposited inside the calorimeter chamber.

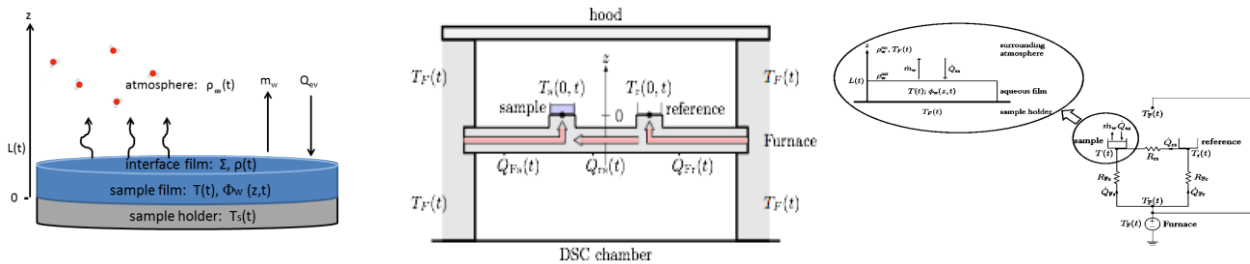


Figure S4. Example of an experimental dehydration curve of aqueous solutions from thin films measured by isothermal calorimetry. The three characteristic regions shown in the experimental curve are resolved in three processes, corresponding to: A) quasi-constant rate (qcr) region (green dot line); B) characteristic sigmoidal shape (blue dot curve); C) initial thermal perturbation of the calorimeter (red dot peak). The sum of the three processes gives the experimentally determined black curve, which overlaps the “reconstructed” experimental curve (red continuous line) corresponding to the actual evaporation process $HF(t)$.

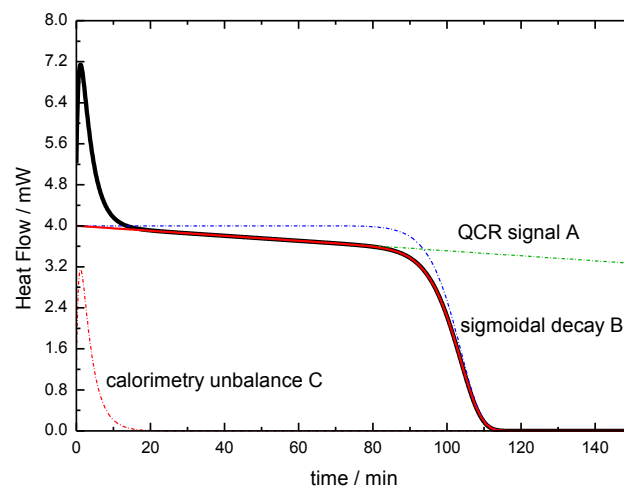


Figure S5. Ultraviolet Brillouin Scattering: Typical IUVS spectrum. Data points (dots) refer to PEG 600 solution (at $x=0.33$ $T=85$ °C). The elastic (red line) and inelastic (green line) contributions together with the resulting best fit (blue line) are indicated. Light black line indicates the experimental resolution.

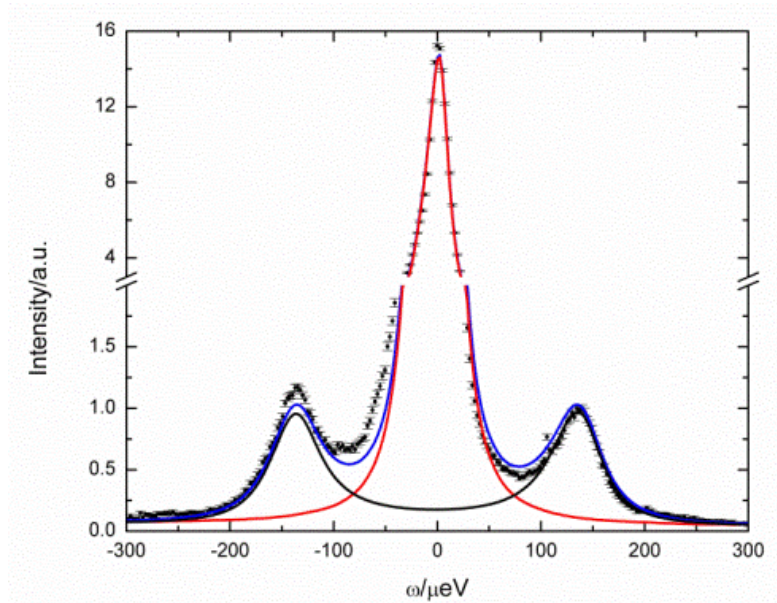


Figure S6. Characteristic temperature, T_M , (square symbols) and T_g as a function of the monomer molar fraction x . The linear T_g line (Gordon-Taylor equation with $k=1$) has been drawn by using the literature values for water [1] and for PEG [2]. The T_M data point show a curvature as previously found for sugar solutes [3]. It is argued that a similar curvature could be shown by the T_g line.

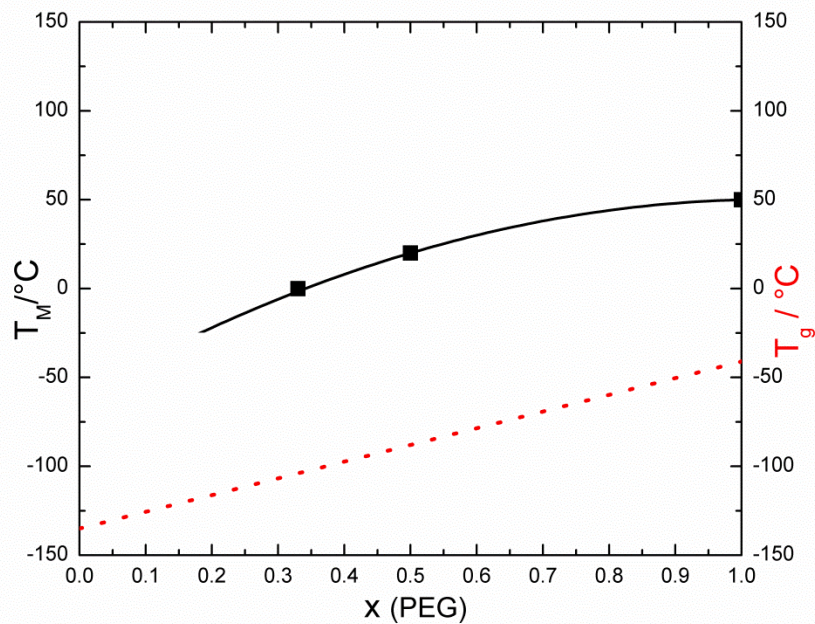
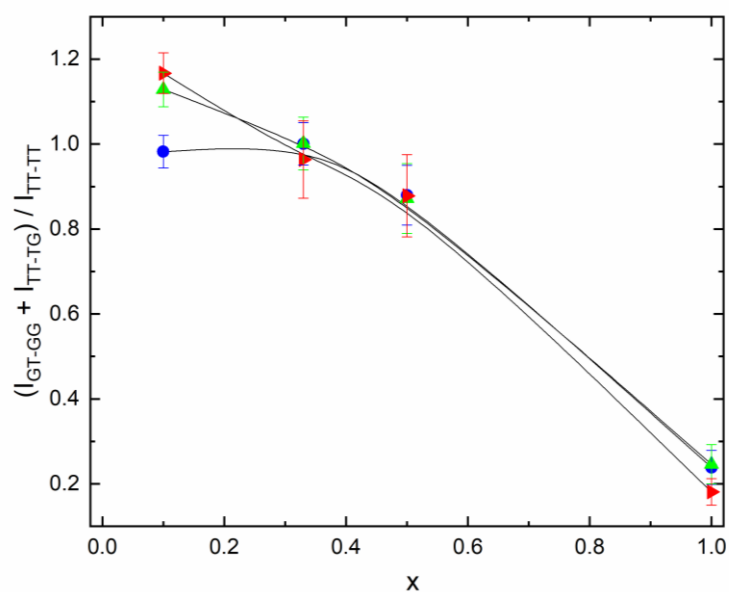


Figure S7. Raman Intensity ratio $(I_{GTGG} + I_{TT-TG})/I_{TT-TT}$ as a function of monomer molar fraction of PEG 600 aqueous solution. Blue circles 27 °C, green triangles 57 °C, red triangles 87 °C.



References

1. Angell, C.A. & Sare, E.J. (1970). Glass-forming composition regions and glass transition temperatures for aqueous electrolyte solutions. *J.Chem. Phys.* 52, 1058–1068.
2. Faucher, J. A., Koleske, J. V., Santee Jr, E. R., Stratta, J. J., & Wilson III, C. W. (1966). Glass transitions of ethylene oxide polymers. *Journal of Applied Physics*, 37(11), 3962-3964.
3. Di Fonzo, S., Masciovecchio, C., Gessini, A., Bencivenga, F., & Cesàro, A. (2013). Water Dynamics and Structural Relaxation in Concentrated Sugar Solutions. *Food Biophysics*, 8(3), 183-191.